Monatsh Chem (2013) 144:1775–1782
DOI 10.1007/s00706-013-1063-y

ORIGINAL PAPER

Flower-like morphology of poly(*m*-aminobenzoic acid) deposited at GC surface in the presence of silica nanoparticles: electropolymerization and characterization

Ali Rostami · Abdollah Omrani · Nooshin Hamedian

Received: 27 February 2013 / Accepted: 16 July 2013 / Published online: 17 September 2013

Abstract Poly(*m*-aminobenzoic acid) film is deposited on glassy carbon electrode by electropolymerization at pH 6.0 in phosphate buffer solutions. The electrochemical behavior of the polymer film is characterized by cyclic voltammetry, electrochemical impedance spectroscopy, Fourier-transform infrared spectroscopy, and scanning electron microscopy. The effect of the scan rate on the peak current is investigated in the range of 50–200 mV/s, indicating that both the anodic and cathodic peak currents increased with the solution pH until 8 and then decreased. Characteristic absorption features related to benzenoid and quinoid and various types of C–N bonds are analyzed.

Keywords Aminobenzoic acid · Electropolymerization · Scanning electron microscopy · Electrochemical impedance spectroscopy

Introduction

Chemically modified electrodes (CMEs) have become an exciting field of research due to their unique electrode surface properties [1]. Many techniques have been developed for preparation of modified electrodes, such as covalent bonding and polymer film formation [2]. Depositing a film of conducting polymer at the electrode surface in an electrolyte medium has been shown to be essential due to electrode surface protection and subsequent prevention, delaying the electropolymerization process [3]. Polymeric films possess three-dimensional extensity, a large number of reactive sites, and good stability, and offer the possibility to be designed with particular redox-active sites. On the other hand, electropolymerization is a good technique for immobilizing polymeric films on electrode surfaces and is privileged due to its unique control over film thickness and charge transport properties [4]. In this respect, numerous monomers, such as thiophene, pyrrole, aniline [5, 6], *o*-, *m*-, and *p*-aminobenzoic acid and their copolymers [7–10], and others [11], have been synthesized electrochemically on different metallic or nonmetallic substrates such as glassy carbon, gold, copper, and aluminum [12, 13].

Also, a deposition mechanism proposed by Hillman and coworkers involves instantaneous nucleation and three-dimensional (3D) growth of nuclei until they overlap, leading to the formation of polymeric film [14]. Various measurement techniques have been applied to investigate the electrochemical polymerization of *m*-aminobenzoic acid and its derivatives, most studies being performed under potentiostatic control using the potential pulse and potential sweep techniques, while other measurement techniques including conductivity measurements, ultraviolet–visible (UV–Vis) spectroscopy, and electrochemical impedance spectroscopy (EIS) [15] have also been utilized recently. Kinetic studies of electroactive polymer films, including both redox and conducting polymers, have been carried out by impedance spectroscopy, while the effects of various parameters such as the solvent [16], electrolyte, and temperature on the mechanical strength, stability, and conductivity of polymer films have also been investigated

A. Rostami (✉)
Faculty of Science, Department of Chemistry, Shahid Beheshti University, 1983963113 Evin, Tehran, Iran
e-mail: arostami.sbu@gmail.com

A. Omrani (✉) · N. Hamedian
Faculty of Chemistry, University of Mazandaran, P.O. Box 453, Babolsar, Iran
e-mail: omrani@umz.ac.ir

[17]. In recent years, metal nanoparticles have attracted much more attention in electroanalysis owing to their unusual physical and chemical characteristics [18–20]. Many nanomaterials including TiO_2 nanostructured films [21], carbon nanotubes [22–26], carbon nanofibers [27, 28], mesoporous carbon [29], and gold nanoparticles (GNPs) [30] have been employed to modify the electrode surface, while silicate films and composite materials have also been utilized, being prepared by the sol–gel method [31]. This methodology provides a cryochemical approach to both design and control the microstructure of such materials. Electrodes modified with metal nanoparticles, especially noble-metal nanoparticles, usually exhibit high electrocatalytic activities towards compounds that show sluggish redox processes at bare electrodes. As the most stable noble-metal nanoparticles, GNPs have increasingly been used in many electrochemical applications, since they exhibit the ability to enhance the electrode conductivity and facilitate electron transfer, thus improving the analytical performance [17].

In the present work, *m*-aminobenzoic acid was selected as the monomer to perform electrochemical polymerization in phosphate buffer solution (PBS). Cyclic voltammetry (CV) was used to deposit polymeric films on glassy carbon electrode (GCE) as the working electrode. Also, *m*-aminobenzoic contains electron-rich N atom and carbonyl group with high electron density, facilitating polymerization on the GC surface. Among the various nanoparticles, preparation of silica–conducting polymer composites is of particular interest, because the surface of silica nanoparticles can easily be altered to accommodate specific catalytic, magnetic, electronic, optical or optoelectronic properties. In addition, these hybrid materials combine the properties of the conducting polymer and the high colloidal stability of the silica, which could significantly widen their applicability in various fields. The silica may act as a template for adsorption of *m*-aminobenzoic acid (*m*-ABA) monomers as well as counterions for doping of the synthesized *m*-ABA. The role of synthetic parameters such as scan rate and pH was addressed, and the conductivity and electropolymerization mechanism of the *m*-aminobenzoic acid and *m*-aminobenzoic acid/SiO_2 systems were also investigated.

Results and discussion

Electropolymerization of m-ABA on GCE surface

Figure 1 shows cyclic voltammograms recorded during oxidative polymerization of 1.0×10^{-3} M *m*-aminobenzoic acid from −1.5 to 2.5 V at scan rate of 100 mV/s for 50 cycles in pH 6.0 PBS on GCE. In the first scan, anodic current peak 1 was observed with current value of 261 μA and potential value of 1.52 V, while larger peaks were observed upon continuous scanning, reflecting continuous growth of the film. The film growth was faster for the first cycles than for the other cycles, and from the seventh cycle, the film showed hardly any growth with maximum peak current of 596 μA, indicating saturation of the polymerization process and *m*-ABA deposition on the GCE surface.

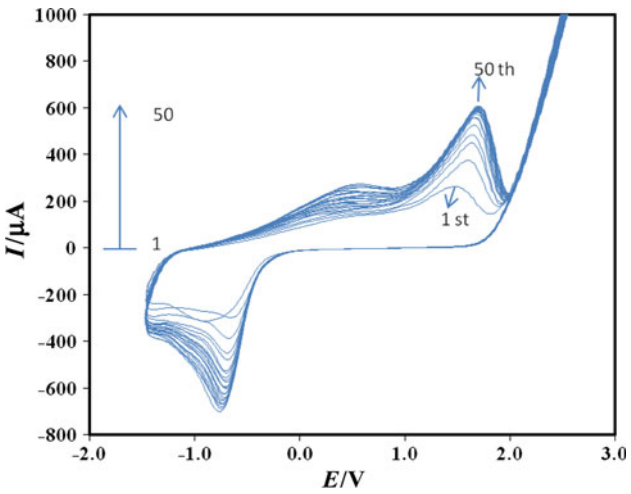

Fig. 1 Cyclic voltammograms of 1.0×10^{-3} M *m*-ABA in pH 6.0 PBS; potential range −1.5 to 2.5 V, scan rate 100 mV/s for 50 cycles at GC electrode

The mechanism of electrochemical polymerization of the monomer is believed to proceed via a radical cation which reacts with a second radical cation to give a dimer [32]. It seems that the first step involves formation of a radical cation [33], and then this intermediate forms a dimeric species by *para*-coupling with either an unoxidized monomer or another radical cation, giving rise to propagation of the reaction (Scheme 1). This mechanism (involving *para*-coupling) is assumed to be valid for oxidative polymerization of *m*-aminobenzoic acid.

Oxidative doping of *m*-ABA may proceed through the following pathway: An electron is removed from the π-system of the backbone, producing a free radical and a spinless positive charge. The radical and cation are coupled to each other via local resonance of the charge and the radical. The combination of a charge site and a radical is called a polaron. This could be either a radical cation or radical anion. Upon further oxidation, the free radical of the polaron will be removed, creating a new spinless defect called a bipolaron. This has lower energy than the creation of two distinct polarons. The formation of polaron and bipolaron species will strongly depend on the level of doping, which is clearly affected by the electropolymerization condition. At higher doping levels, polarons are replaced with bipolarons. Since the bandgap character of these species is different, their availability will control the voltammetric behavior of the *m*-ABA response (Scheme 1).

Scheme 1

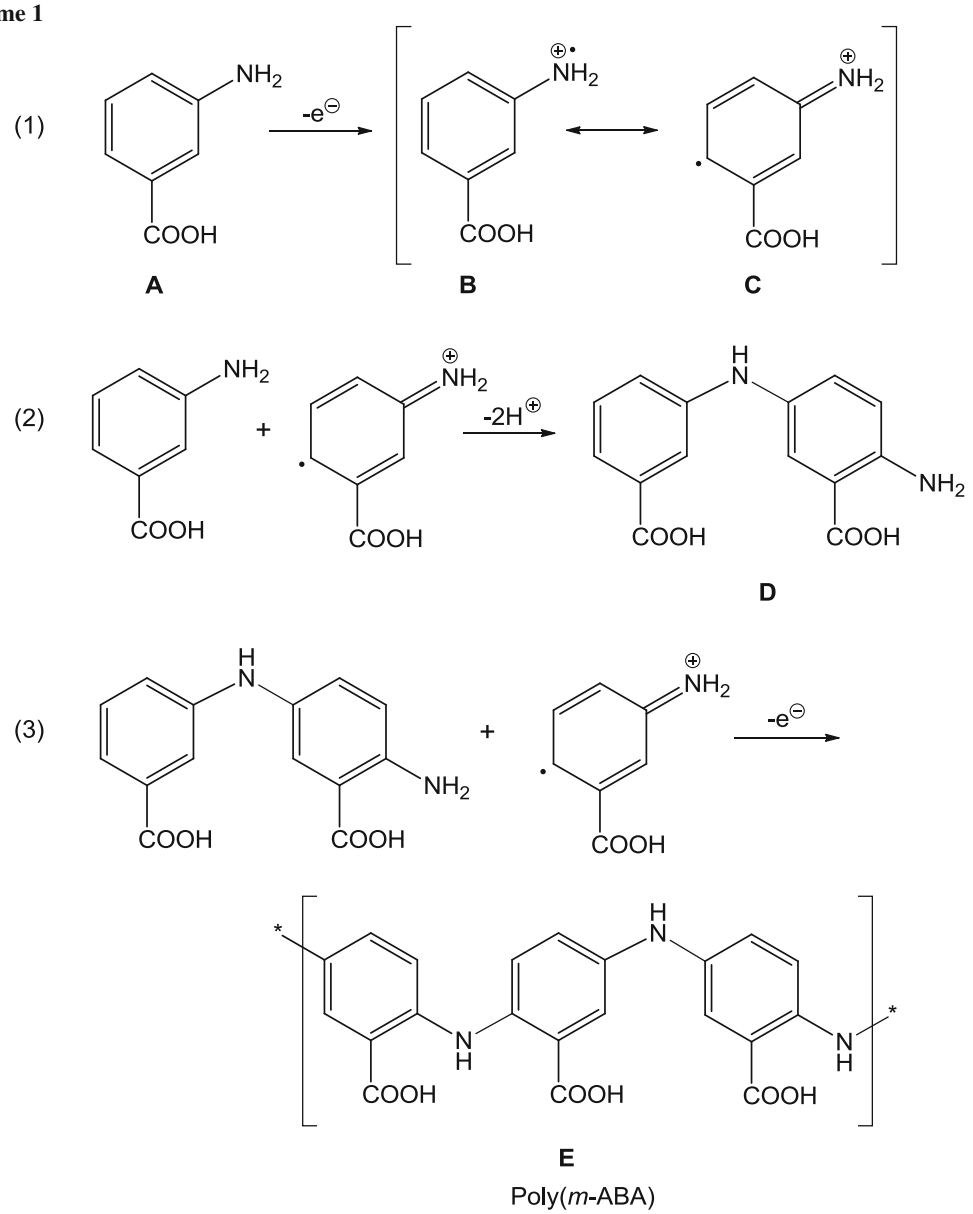

Effect of solution pH on the anodic current peak

The effect of solution pH on the formation of polymeric film was investigated over the range of 3–11. Anodic and cathodic peak currents increased with solution pH until 8, then subsequently decreased until the solution pH reached 11 (Fig. 2).

Effect of scan rate on the anodic peak current

The effect of scan rate on the peak current was investigated in the range of 50–200 mV/s in pH 6.0 PBS on GCE. The anodic peak current was proportional to the scan rate: the peak current enlarged at higher scan rates (Fig. 3) due to rapid diffusion of *m*-ABA monomer to the electrode surface. Also, the anion of the electrolyte may dope the positively changed species formed during the electropolymerization of *m*-ABA faster as the scan rate increased.

Electrochemical impedance characterization of poly(m-ABA)-modified electrode

As is well known from measurements performed under potential control, the low-frequency impedance of polymer-covered electrodes can be approximated by a limiting low-frequency capacitance and a series resistance [34, 35].

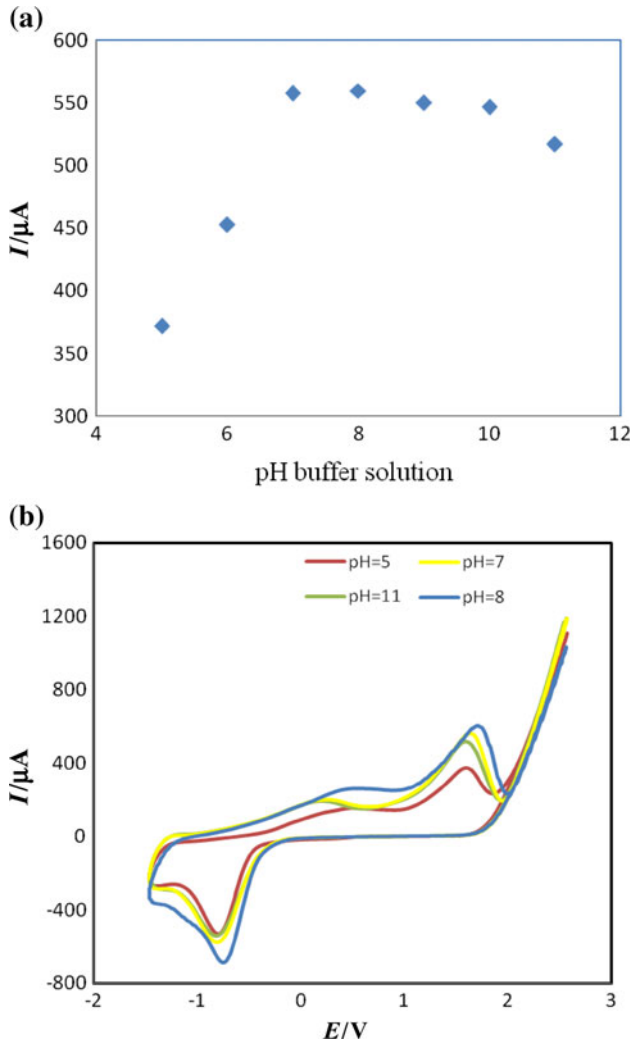

Fig. 2 Effect of pH on the anodic peak current (**a**, **b**); scan rate 100 mV/s

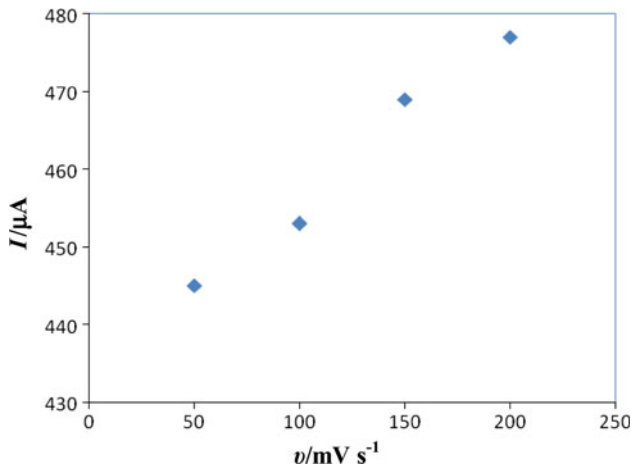

Fig. 3 Effect of scan rate on the anodic peak current peak in pH 6.0 PBS

EIS experiments were carried out in 5.0×10^{-3} M $[Fe(CN)_6]^{-3}/[Fe(CN)_6]^{-4}$ solution. Figure 4 and Table 1 summarize the respective data related to the modified GC electrodes. The results from the Nyquist profiles in Fig. 4 indicate that the charge-transfer resistance (R_{ct}) of the polymeric film is increased due to the electrochemical polymerization of *m*-ABA in the presence of SiO_2 nanoparticles. The embedding of nonconductive SiO_2 nanoparticles within the polymer matrix may be responsible for the increment of R_{ct} and observed reduced conductivity.

The impedance plots were analyzed using an equivalent electrical circuit, where R_s represents the electrolyte resistance, R_c is the coating pore resistance with poly(*m*-ABA), and C_c is the coating capacitance. Figure 4c shows the Randle-type circuit used for the simulation process. The quality of fitting was judged by limiting the relative error in the value of each element in the equivalent circuit to a maximum of 5 %.

Spectroscopic characterization of the produced poly(m-ABA) film

Figure 5 shows the FT-IR spectrum of the film produced in PBS. The band around 3,300–3,450 cm^{-1} is attributed to characteristic N–H stretching vibration, while the band

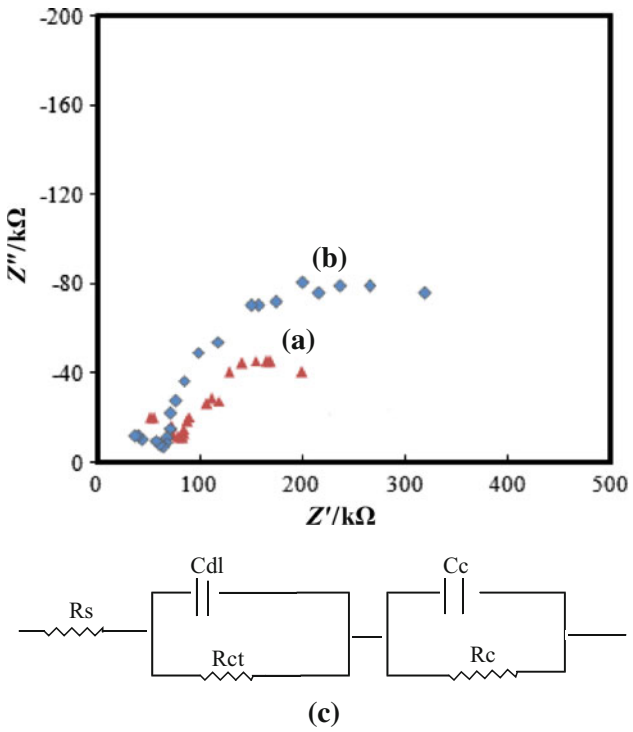

Fig. 4 Nyquist impedance plots of *a* modified electrode, *b* modified electrode with SiO_2 nanoparticles, and *c* the corresponding equivalent electrical circuit

Table 1 Impedance parameters determined by fitting experimental data using an appropriate equivalent circuit for the GC/*m*-ABA and GC/*m*-ABA/SiO_2 systems

Sample	R_{ct}/Ω cm^{-2}	R_c/Ω cm^{-2}	R_s/Ω cm^{-2}
GCE/*m*-ABA	49.6	179.4	64.2
GCE/*m*-ABA/SiO_2	68.2	275.1	68.3

observed at 1,650 cm^{-1} is related to carbonyl group vibration in the carboxylic acid moiety. The band appearing at 1,150 cm^{-1} is related to single-band aromatic C–N stretching of secondary aromatic amines [36]. These diagnostic vibrational bands also support the proposed mechanism of the electropolymerization process mentioned above.

It should be noticed that the preservation of the carboxylic group in the chemical structure of poly(*m*-aminobenzoic acid) is evidenced by the existence of the 1,700 cm^{-1} (reduced form) and 1,729 cm^{-1} (oxidized form) absorption bands [12]. The considerable shift, as seen in Fig. 5, in the peak frequency for this band to 1,650 cm^{-1} may be due to the presence of the silica nanoparticles and/or chemical interaction between the carboxylic and amino groups in the reduced state of poly(*m*-aminobenzoic acid). Also, the disappearance of the signal corresponding to C=C stretching at about 1,500 cm^{-1} demonstrates the transformation from benzenoid rings to quinoid structures.

Surface analysis of deposited poly(m-ABA)

SEM images of the electrodeposited poly(*m*-ABA) film and poly(*m*-ABA)/SiO_2 nanocomposite are shown in Fig. 6. The polymer was formed using the cyclic voltammetry technique during 25 cycles. In Fig. 6a, b, the poly(*m*-ABA) films appear to be thin on the carbon electrode surface, exhibiting flower-like hierarchical structures with size ranging from 4 to 10 μm, forming compact assembled irregular sheets. Surprisingly, in sodium acetate solution (Fig. 6c), the film morphology changed to granular with greater thickness.

Effect of SiO_2 nanoparticles on poly(m-ABA) deposition

Cyclic voltammograms (CVs) were recorded during oxidative polymerization of *m*-aminobenzoic solution (1.0×10^{-3} M) in a suspension of SiO_2 nanoparticles in PBS (pH 6.0). As can be seen in Fig. 7, during the first scan, an anodic peak current was observed with current value of 132 μA at 1.55 V, and upon continuous scanning, the corresponding signal increased, reflecting continuous growth of the film. During deposition of poly(*m*-ABA)/SiO_2 on the GC surface, as the number of cycles increased, the peak currents increased accordingly. Apparently, these current values are lower than for electropolymerization of *m*-ABA in the absence of silica nanoparticles (Fig. 1). The maximum peak current value observed during the electropolymerization process was around 520 μA; moreover, it is also interesting to note that the voltammetric charge decreases with increasing SiO_2 content.

Cyclic voltammograms of *m*-ABA- and *m*-ABA/SiO_2-modified electrodes and the corresponding peak currents were compared at the 50th cycle. These results indicated that the conductivity of the polymeric film decreased in the presence of SiO_2 nanoparticles (Fig. 8).

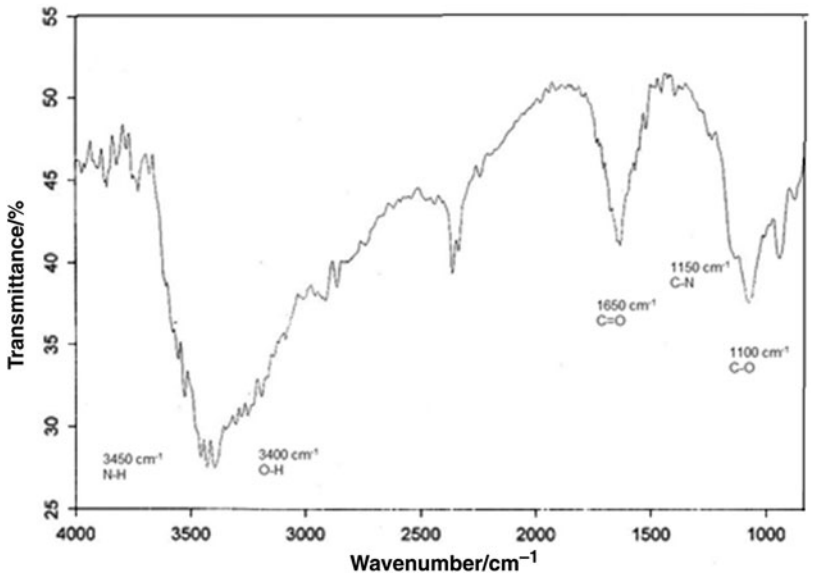

Fig. 5 FT-IR spectrum of the poly(*m*-aminobenzoic acid) coating synthesized on GC substrate using cyclic voltammetry technique

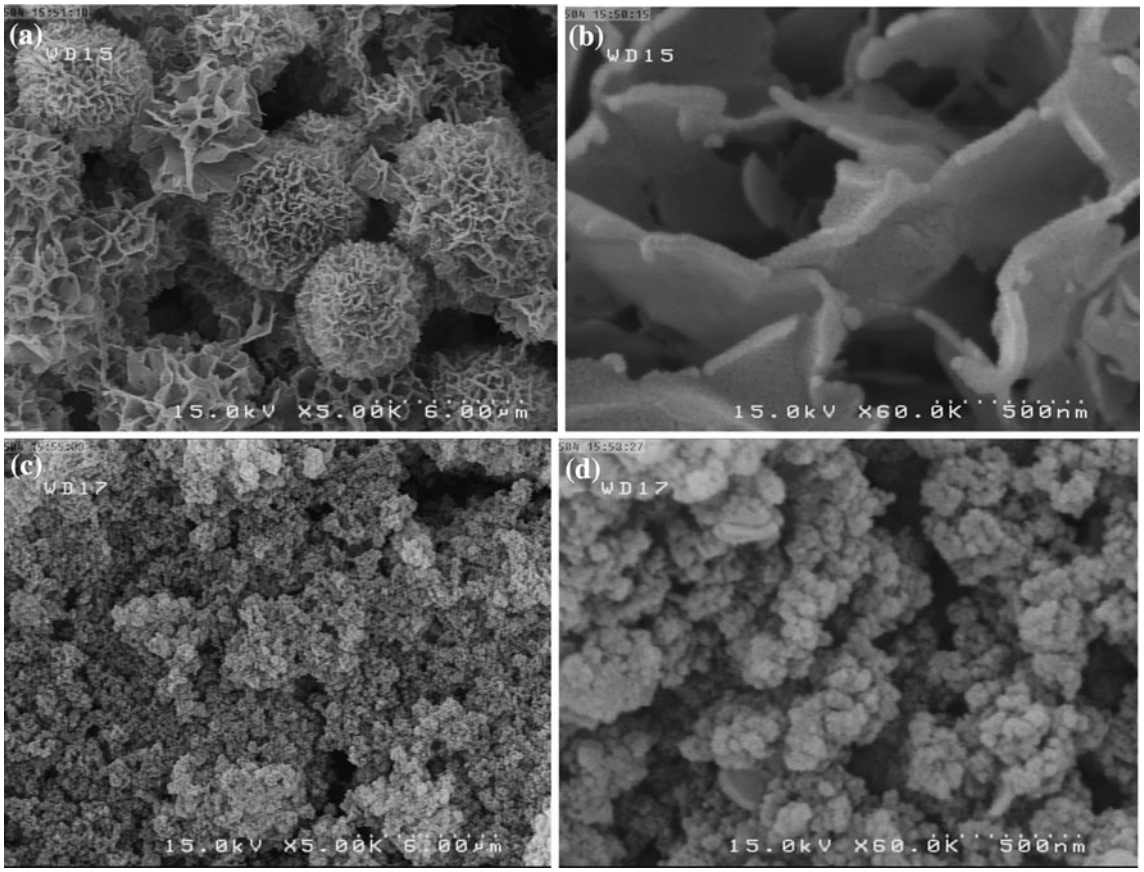

Fig. 6 SEM images of coatings synthesized on GC: *a*, *b* *m*-ABA, and *c*, *d* *m*-ABA/SiO_2 systems at various magnifications

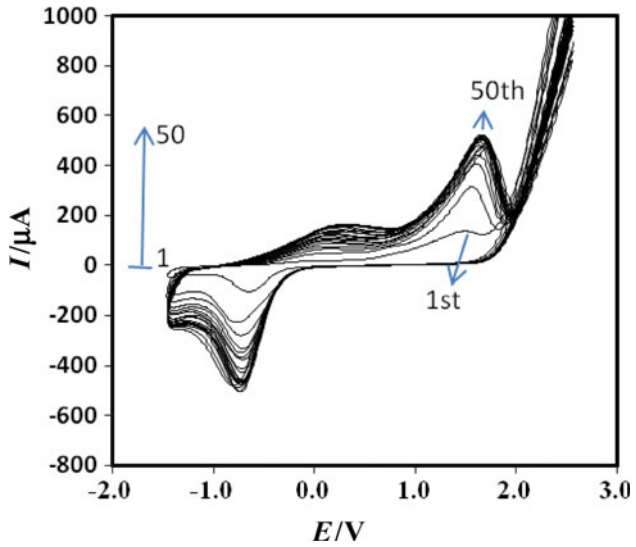

Fig. 7 Cyclic voltammograms of 1.0×10^{-3} M *m*-ABA with SiO_2 nanoparticles in pH 6.0 PBS; potential range −1.5 to 2.5 V, scan rate 100 mV/s for 50 cycles on GC electrode

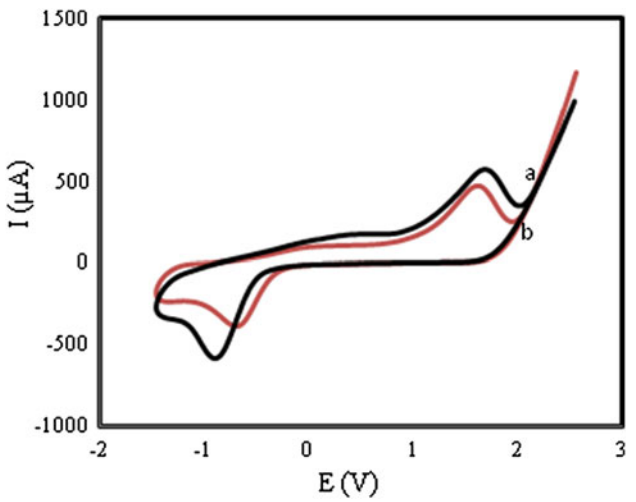

Fig. 8 Fifty cyclic voltammograms of *a* *m*-ABA, and *b* *m*-ABA/SiO_2 systems on GC electrode

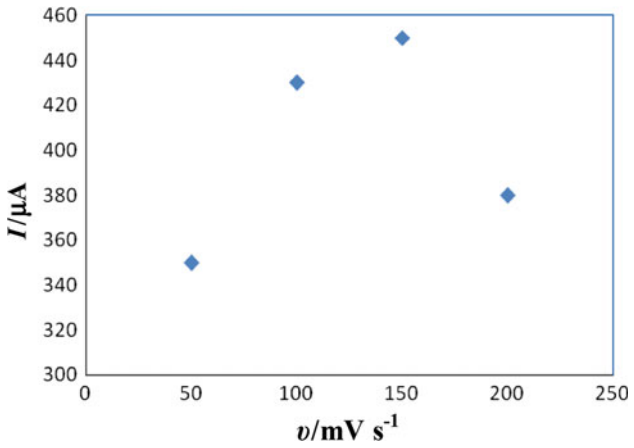

Fig. 9 Effect of scan rate on the anodic peak current of the coating with SiO_2 nanoparticles at pH 6.0 PBS

Effect of scan rate on deposition of the poly(m-ABA)/ SiO_2 system

The effect of scan rate on the anodic peak current was investigated in the range of 50–200 mV/s. From the results, shown in Fig. 9 and, it is clear that the anodic peak current shifted in the positive direction at higher scan rates up to 150 mV/s, but then decreased at 200 mV/s. These observations indicate that there could be a limitation on the electroactive species reaching the GC electrode surface for high scan rates, with a corresponding decrease in Faradic current.

Conclusions

Cyclic voltammetry was used to synthesize poly(*m*-aminobenzoic acid) films at a GCE surface. The redox behavior of the obtained films was investigated in the presence of silica nanoparticles. Poly(*m*-aminobenzoic acid) showed two separate voltammetric processes, which may be attributed to the formation of polaronic and bipolaronic species. The effect of solution pH on the electrochemical behavior of poly(*m*-aminobenzoic acid) was also investigated. Results indicated that the presence of the –COOH group attached to the polymer backbone preserved most of its electrochemical response, i.e., oxidation–reduction characteristics, at pH values typically >6. FT-IR spectroscopy studies confirmed the *para*-coupling mechanism, and EIS studies revealed that the electron-transfer resistance of the polymeric film was increased with increasing loading level of SiO_2 nanoparticles.

Experimental

m-Aminobenzoic acid (Fluka AG, Buchs SG, Switzerland) was utilized as monomer. Silica nanoparticles (purity >99.5 %) were purchased from Aldrich (Germany) with average size of 10–20 nm, confirmed by transmission electron microscopy (TEM). PBS with pH 6.0 was prepared from 0.1 M NaH_2PO_4–Na_2HPO_4 and used as electrolyte.

Cyclic voltammetry (CV) studies were carried out on an EG&G (USA) model 263 A potentiostat/galvanostat with a personal computer (PC) and electrochemical setup using M270 software. Electrochemical impedance spectroscopy measurements were performed using an EG&G (USA) model 1025 frequency response detector with a PC and electrochemical setup controlled by M398 software. The FT-IR transmission spectrum of the *m*-ABA coating was recorded in horizontal attenuated total reflectance mode in the spectral range of 550–3,500 cm^{-1} using a Bruker (Germany) Vector series 22 spectrometer. Scanning electron microscopy (SEM) images were taken using a VEGA HV (high potential) 1,500 V at various magnifications.

Cell and electrodes

A conventional three-electrode system was employed with a bare or poly(*m*-ABA)-modified glassy carbon electrode (GCE) (1.0 mm diameter) as the working electrode, a Ag/AgCl (KCl: 3 M) electrode as the reference electrode, and a platinum electrode considered as the counterelectrode. Before each electrochemical experiment, the working electrode was mechanically polished with abrasive paper (2,400 grade), then rinsed with distilled water, and finally dried under argon flow. After deposition, the working electrode was removed from the electrolyte, rinsed with double-distilled water, and finally dried in air. All measurements were carried out at room temperature.

Electropolymerization

Electropolymerization solution consisting of 1.0×10^{-3} M *m*-ABA was added to phosphate buffer as electrolyte solution. Electrochemical studies were conducted using the potentiodynamic polarization technique in buffer solutions. The film was deposited on the electrode by cyclic sweeping from −1.5 to 2.5 V at 50, 100, 150, and 200 mV/s for 10, 20, and 50 cycles in pH 6.0 PBS containing 1.0×10^{-3} M *m*-ABA. The same preparation procedure was used to deposit poly(*m*-ABA) films from suspension solution containing SiO_2 nanoparticles. EIS measurements were performed in the presence of 5.0×10^{-3} M $[Fe(CN)_6]^{-3}$/$[Fe(CN)_6]^{-4}$ as redox probe. An alternating-current (ac)

voltage with 5 mV amplitude in the frequency range from 50 mHz to 65 kHz was superimposed on the direct-current (dc) potential and applied to the studied electrode. The dc potential was always set up at the formal potential of $[Fe(CN)_6]^{-3}/^{-4}$.

References

1. Cheng W, Jin G, Zhang Y (2005) Russ J Electrochem 41:940
2. Daum P, Murry RW (1981) J Phys Chem 85:389
3. Sharifirad M, Omrani A, Rostami AA, Khoshroo M (2010) J Electroanal Chem 645:149
4. Kaya I, Bilici A (2010) Polym Adv Technol 21:337
5. Benyoucef A, Boussalem S, Belbachir M (2009) World J Chem 4:171
6. Dalmolin C, Canobre SC, Biaggio SR, Rocha-Filho R, Bocchi N (2005) J Electroanal Chem 578:9
7. Zhang Y, Wang J, Xu M (2010) Colloid Surf B 75:179
8. Thiemann C, Brett CMA (2001) Synth Met 123:1
9. Brett CMA, Thiemann C (2002) J Electroanal Chem 538–539:215
10. Benyoucef A, Huerta F, Vázquez JL, Morallon E (2005) Eur Polym J 41:843
11. Tanguy J (2000) J Electroanal Chem 487:120
12. Benyoucef A, Huerta F, Ferrahi MI, Morallon E (2008) J Electroanal Chem 624:245
13. Rudge A, Raistrick J, Gottesfeld S, Ferraris P (1994) Electrochim Acta 39:273
14. Hillman AR, Mallen EF (1987) J Electroanal Chem 220:351
15. Sundfors F, Bobacka J (2004) J Chem 572:309
16. Yao H, Sun Y, Lin X, Tang Y, Huang L (2007) Electrochim Acta 52:6165
17. Sayyah SM, El-Rabiey MM, Abd El-Rehim SS, Azooz RE (2008) J Appl Polym Sci 109:1643
18. Shi H, Xu Y, Wang Y, Song W (2010) Microchim Acta 171:81
19. Haldorai Y, Long PQ, Noh SK, Lyoo WS, Shim JJ (2011) Polym Adv Technol 22:781
20. Liu X, Li B, Wang X, Li C (2010) Microchim Acta 171:399
21. Curulli A, Valentini E, Padeletti G, Viticoli A, Caschera D, Palleschi G (2005) Sens Actuators B Chem 111:441
22. Wang J, Musameh M (2003) Anal Chem 75:2075
23. Tsai YC, Huang JD, Chiu CC (2007) Biosens Bioelectron 22:3051
24. Zhang MG, Gorski W (2005) J Am Chem Soc 127:2058
25. Zhai XR, Wei WZ, Zeng JX, Gong SJ, Yin J (2006) Microchim Acta 154:315
26. Wu BY, Hou SH, Yin F, Zhao ZX, Wang YY, Wang XS (2007) Biosens Bioelectron 22:2854
27. Wu LN, Zhang XJ, Ju HX (2007) Anal Chem 79:453
28. Arvinte A, Valentini F, Radoi A, Arduini F, Tamburri E, Rotariu L, Palleschi G, Bala C (2007) J Electroanal Chem 19:1455
29. Wang Y, You CP, Zhang S, Kong JL, Marty JL, Zhao DY, Liu BH (2009) Microchim Acta 167:75
30. Jena BK, Raj CR (2006) Anal Chem 78:6332
31. Li J, Chia LS, Goh NK, Tan SN (1999) J Electroanal Chem 460:234
32. Alishah AH, Holze R (2006) J Electroanal Chem 597:95
33. Bard AJ, Yang H (1992) J Electroanal Chem 339:423
34. Macdonald DD (2006) Microchim Acta 51:1376
35. Khoshroo M, Rostami AA (2010) J Electroanal Chem 647:117
36. Salvagione HJ, Acevedo DF, Miras MC, Motheo AJ, Barbero CA (2004) J Polym Sci Part A Polym Chem 42:5587